Revista Brasileira de Cartografia
ISSN 1808-0936 | https://doi.org/10.14393/revbrascartogr
Sociedade Brasileira de Cartografia, Geodésia, Fotogrametria e Sensoriamento Remoto

Classification of Potential Wetlands using the Random Forest in Google Earth Engine in Geomorphological Units - Rio Grande do Sul, Brazil

Classificação de área úmidas potenciais usando Random Forest no Google Earh Engine em Unidades Geomorfológicas – Rio Grande do Sul, Brasil

Christhian Santana Cunha [1], Laurindo Antonio Guasselli [2], Tássia Fraga Belloli [3] e Carina Cristiane Korb[4]

1 Universidade Federal do Rio Grande do Sul, Porto Alegre, Brasil. christhianscunha@gmail.com
ORCID: https://orcid.org/0000-0002-0755-6760
2 Universidade Federal do Rio Grande do Sul, Porto Alegre, Brasil. laurindo.guasselli@ufrgs.br
ORCID: https://orcid.org/0000-0001-8300-846X
3 Universidade Federal do Rio Grande do Sul, Porto Alegre, Brasil. tassiabellolif@gmail.com
ORCID: https://orcid.org/0000-0001-6365-7796
4 Universidade Federal do Rio Grande do Sul, Porto Alegre, Brasil. carinac.korb@gmail.com
ORCID: https://orcid.org/0009-0007-9954-2043

Recebido: 06.2023 | Aceito: 09.2023

Abstract: Wetlands are important and valuable ecosystems in the landscape of the extreme south of Brazil. However, they are among the ecosystems threatened by human pressures and climate change. Monitoring and managing these environments is a challenge due to their high spatial and temporal dynamics. The use of remote sensing techniques, supervised classification, and machine learning algorithms offers a promising opportunity to map and monitor wetlands. The objective of this work is to develop a method to map Potential Wetlands (PW) from the integration of images from different satellites, sensor systems, spectral, topographic, climatological and hydrological features, made available on the Google Earth Engine (GEE) cloud user platform. Supervised classification was performed on the geomorphological units Coastal Plain (CP) and Central Depression (CD) considering two classes: Potential Wetlands, which encompasses all types of wetlands, and No Wetlands, for the remaining land use and occupation classes. The supervised pixel-by-pixel classification, individual for each geomorphological unit, allowed more accurate results consistent with previous, consolidated mapping. The PW were mapped with a global accuracy higher than 88% and consumer and producer accuracy higher than 81% in the Coastal Plain and Central Depression. These results allow us to affirm that the proposed methodology enabled the identification of 22% to 24% increase in potential wetlands in geomorphological regions, from spectral signatures, and pixel-by-pixel supervised classification of PW using different image collections and sensor systems.
Keywords: Wetlands; Google Earth Engine; Random Forest.

Resumo: As áreas úmidas são ecossistemas importantes e valiosos na paisagem do extremo sul do Brasil. No entanto, eles estão entre os ecossistemas ameaçados pelas pressões humanas e pelas mudanças climáticas. O uso de técnicas de sensoriamento remoto, classificação supervisionada e algoritmos de aprendizado de máquina oferece uma oportunidade promissora para mapear e monitorar áreas úmidas. O objetivo deste trabalho é desenvolver um método para mapear Áreas Úmidas Potenciais (AP) a partir da integração de imagens de diferentes satélites, sistemas de sensores, feições espectrais, topográficas, climatológicas e hidrológicas, disponibilizadas na plataforma Google Earth Engine. A classificação supervisionada e o mapeamento foram realizados para as unidades geomorfológicas Planície Costeira (PC) e Depressão Central (DC) considerando duas classes: Áreas Úmidas Potenciais, que engloba todos os tipos de áreas úmidas, e Áreas Não Úmidas, para as demais classes. A classificação, individual para cada unidade geomorfológica, permitiu resultados acurados frente a bases oficiais. As APs foram mapeadas com acurácia global superior a 88% e acurácia do consumidor e produtor superior a 81% na PC e DC. Esses resultados demonstram que a metodologia proposta possibilitou a identificação do aumento de 22% a 24% em áreas úmidas potenciais nas regiões geomorfológicas estudadas.
Palavras-chave: Áreas úmidas; Google Earth Engine; Random Forest.

1 INTRODUCTION

Wetlands are being drastically converted into non-wetland habitats due to agricultural activities (VOLK et al., 2017; ZOU et al., 2018), urbanization (ALIKHANI; NUMMI; OJALA, 2021), natural processes, and climate change impacts (TINER; LANG; KLEMAS, 2015; MOOMAW et al., 2018). They are among the ecosystems that experience the greatest anthropogenic pressure, even though they play a vital role for humans (SMARDON, 2014; MOOMAW et al., 2018).

Despite the benefits of Wetlands, comprehensive inventories are lacking in most countries due to the high investments with mapping, the high dynamics and remote nature of these ecosystems (GALLANT, 2015; HALABISKY, 2019).

These issues result in partial, fragmented, or outdated inventories. Some countries do not even have inventories available (MAXA; BOLSTAD, 2009; MAHDIANPARI et al., 2019).

Wetlands are defined as water-saturated habitats that create hydric soil suitable for the growth of water-tolerant plants (RUBEC, 2018; JAMALI et al., 2021). Wetlands mappings and classifications generally follow two trends. Horizontal classifications divide habitats into a series of classes or types, such as salt marshes, peatlands, mangroves, etc. (FRANKLIN et al., 2018; KAPLAN; AVDAN, 2019; MAHDIANPARI et al., 2020). Hierarchical classifications separate Wetlands types into different levels and, are most commonly used in inventories (OLLIS et al., 2013; MEDDE, 2014; MAO et al., 2020; SALINAS et al., 2020). This approach facilitates regional, national, and international comparisons between similar systems and allows for greater detail of individual types in the landscape (TINER, 1999).

Different criteria are used to define the nature, boundaries, and heterogeneity of Wetlands (MEROT et al., 2006). In addition, several countries have their legislation and official instruments for identification and classification of Wetlands. Among the hierarchical methods, the Cowardin et al. (1979) and Ramsar (SCOTT; JONES 1995) systems have vegetation and hydrology as central classification criteria. Semeniuk; Semeniuk (1995; 2011), Brinson (1993; 2009) and Smith et al. (1995) adopt hydrological and geomorphological parameters. For these authors, vegetation should not be the main or the first classification criterion, due to its dependence on hydrological and geomorphological factors. In addition, some important functions for its maintenance and functioning are independent of vegetation (GOMES; MAGALHÃES JÚNIOR, 2018).

In this context, the growing awareness of the role played by Wetlands in the global climate system (MOOMAW et al., 2018) has led to a proliferation of land surface models (LSM) designed for their quantification. However, these models take different approaches, with disagreements related to their extent in both space and time (HU et al., 2017).

To achieve coherence between different hierarchical delineation methods, Merot et al. (2006) defined a functional approach based on the potential distribution of wetlands. Potential Wetlands (PW) are defined by topographic and pedoclimatic criteria derived from a Digital Elevation Model and a soil database (MEROT et al., 2006), and include those geographic situations where geomorphological or climatic criteria entail a high probability of wetland occurrence (BERTHIER et al., 2014).

PW can be considered as the maximum natural extent of wetlands. They therefore include old wetlands that have already been disturbed as, for example, by artificial drainage, urbanization, or river rectification (RAPINEL et al. 2019). It can be understood as preliminary knowledge, especially in regions where inventories have not yet been conducted, making it readily available for policy managers and providing a comparative framework for wetland inventories (MEROT et al., 2006).

Knowing the potential distribution of wetlands aids in understanding their formation and detecting changes, as well as in decision-making for their restoration and protection (HU et al., 2017). This approach was used in Durand et al.(2000), Steyaert et al. (2007) and Berthier et al. (2014) to generate a mapping of PW in France. Rapinel et al. (2019) used it to propose wetland management and assist in identifying sites where restoration measures should be prioritized.

From a methodological standpoint, it is critical to have accessible and reproducible identification criteria that support multiple scales of analysis and allow for continuous monitoring. Due to the dynamic nature of these ecosystems, conventional mapping to monitor changes over time is difficult and time-consuming, requiring extensive fieldwork over large geographic areas (AYANLADE; PROSKE, 2016; HUANG et al.,

2017; KAPLAN; AVDAN, 2018). Knowledge of the extent and distribution of wetlands through comprehensive monitoring programs is a research frontier with important applications in the conservation and management of these ecosystems, as well as to protect them from further alteration and degradation (VALENTI et al., 2020; HALABISKY et al., 2022).

Remote sensing (BAN; YOUSIF 2016; ASOKAN; ANITHA, 2019) is an efficient tool that can play a fundamental and constructive role in assessing, studying, and measuring the extent of changes in Wetlands, both long-term and large-scale (MABWOGA; THUKRAL 2014; MCCARTHY; MERTON; MULLER-KARGER, 2015). On the other hand, it requires considerable processing and storage capacity, given the volume of information required.

In this regard, the development of cloud computing such as Google Earth Engine (GEE), in open access programs with availability of large volumes of Earth Observation (EO) data, archives, and datasets stored in clouds, and advances in machine learning techniques, allow creating comprehensive and large-scale delineation methodologies (HIRD et al., 2017; MAHDIANPARI et al., 2018; MAHDIANPARI et al., 2019; AHMAD et al., 2020; VALENTI et al., 2020; JAMALI et al., 2021) capable of being adapted to diverse geomorphological and climatic conditions.

The GEE platform is designed to help researchers easily share their results with other researchers, policymakers, NGOs, and the public, and access to planetary-scale satellite data and extensive computing power for image processing and analysis (GORELICK et al., 2017). Considering that mappings are sometimes limited to local scales, GEE enables the expansion of classifications to regional or national areas (VALENTI et al., 2020; JAMALI et al., 2021).

Recent efforts by Bourgeau-Chavez et al., (2015), Mahdianpari et al. (2018; 2019; 2020), Wu et al. (2019), Valenti et al. (2020) and Jamali et al. (2021) using remote sensing data and cloud computing programs have yielded significant advances in Wetlands mapping and monitoring.

In the extreme south of Brazil, in the state of Rio Grande do Sul, a great diversity and abundance of Wetlands occurs, including a diversity of microhabitats that contribute to great richness and abundance of waterbirds (GUADAGNIN; MALTCHIK, 2007; GUADAGNIN; MALTCHIK; FONSECA, et al., 2009; SCHUH; GUADAGNIN, 2018). Rio Grande do Sul has international recognition with two Ramsar sites, the Taim Ecological Reserve and the Lagoa do Peixe National Park (ROLON; ROCHA; MALTCHIK, 2011; RIBEIRO et al., 2021).

With the growing concern of researchers to highlight the importance of these areas, in the ecological, social and microclimatic spheres, and to improve mapping techniques, studies have been developed that address delineation and classification of improved remote sensing techniques, such as object-oriented classification (GUASSELLI; SIMIONI; LAURENT, 2020; SIMIONI et al., 2020; RUIZ et al., 2021), but in small-scale wetlands.

Our proposal, however, is to map potential wetlands on a large scale. According to Tassi and Vizzari (2020), GEE sometimes does not allow object-oriented classification processing at large scales. GEOBIA, which includes both object segmentation and texture analysis of objects, is not yet common in GEE, probably due to the difficulty of concatenating the appropriate functions and adjusting the various parameters to overcome the computational limitations of GEE (TASSI; VIZZARI, 2020).

Existing inventories from remote sensing products, which include the spatial distribution of Wetlands in Rio Grande do Sul, incorporate different data sources, methods and mapping scales, making them of limited use for rigorous monitoring of wetlands (FZB, 2013; SEMA, 2018; SOUZA et al., 2020). Thus, we propose in this study a new approach to delineate PW from remote sensing data, including spectral, topographic, and hydrological features, made available on the Google Earth Engine cloud user platform.

From the data set, we sought to verify the most important variables to identify and delimit the PW in two geomorphological units in the state of Rio Grande do Sul, Brazil.

2 METHODOLOGY

2.1 Study Area

To map the PW, two compartments of geomorphologic units in the State of Rio Grande do Sul were used: Coastal Plain (CP) in Figure 1 and Central Depression (CD) in Figure 2. The spatial distribution of the geomorphological units is shown in Figure 3.

Geomorphology and hydrology are important factors for Wetlands classification (SEMENIUK; SEMENIUK, 1995; 2011) because structuring factors tend to be less dynamic and changeable over time compared to biological ones, which allows categorizing Wetlands into more stable classes, even when they are substantially altered by vegetation or soil removal (GOMES; JUNIOR, 2018). In this sense, it was chosen to consider the geomorphological compartments and units as regions of interest.

The Coastal Plain occupies an area of approximately 33,000 km in the outer coastal portion. It preserves the geological and geomorphological record of the Quaternary (TOMAZELLI; VILLWOCK, 2000) and depositional systems of the Lagoon-Barrier type (VILLWOCK ET AL., 1986; VILLWOCK; TOMAZELLI, 1995), marked by transgressive-regressive events. It is a suite of ecosystems dominated by pioneer plant formations of marine and fluvial influence, and grassland and forest formations (SCHAFER, 2013). Mosaics differentiated by landscape morphology and water availability occur, characterized by sparse vegetation in the dry grasslands and dune areas and lush vegetation in the humid areas of depressions and old dune forests (SCHAFER, 2013).

Figure 1 - Wetland in the Coastal Plain, municipality of Palmares do Sul.

Source: Schafer (2013).

The Central Depression, located in the center of the state, corresponds to an area of low altitudes, represented by Mesozoic sediments of the Paraná Basin and express the process of peripheral erosion from the events of the late Mesozoic and Cenozoic. The geomorphology is characterized by a surface consisting of differentiated patterns of hills with either flat tops or convex tops (SUERTEGARAY; GUASSELLI, 2012). It consists predominantly of areas of cleared fields and pastures, an intensive summer agricultural zone, and an agricultural zone of diversified crops (SPGM, 2021).

Figure 2 - Wetland in the Environmental Preservation Area (EPA) of Banhado Grande.

Source: SEMA (2021).

 DOI: http://dx.doi.org/10.14393/rbcv75n0a-69753

Figure 3 - Geomorphological units: Central Depression (CD) and Coastal Plain (CP) and altimetry, Rio Grande do Sul

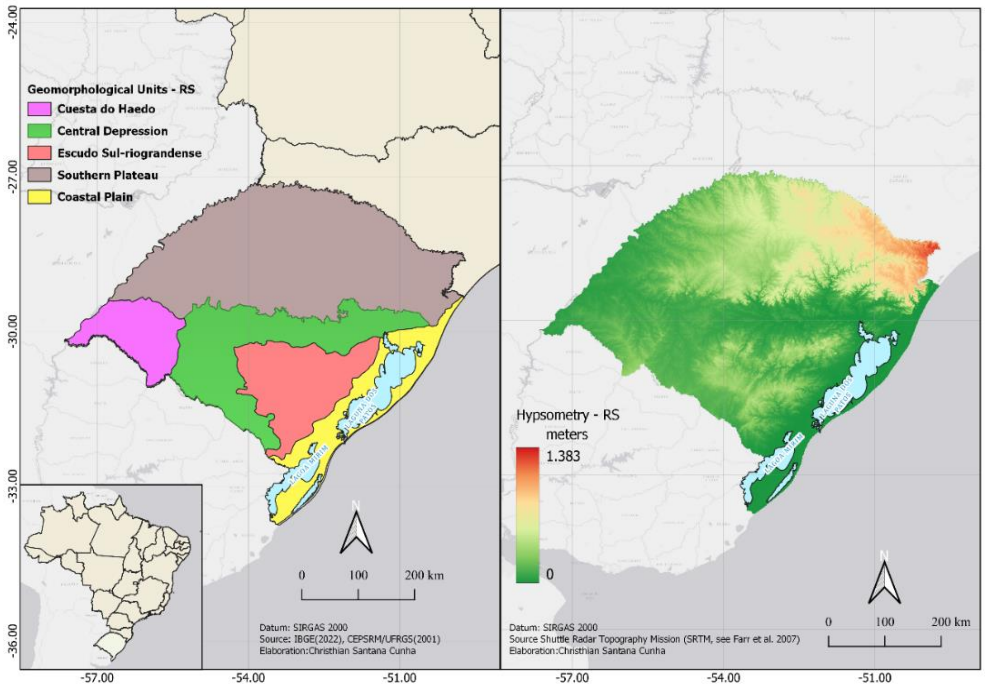

Elaboration: The authors (2023).

2.2 Selection of samples for classification

To determine the number of samples, varying amounts of samples were tested until a sufficient threshold was attained that would enable processing of images and yield satisfactory outcomes. Initial classification tests involved fewer than 8000 samples, but these yielded unacceptable results due to the heterogeneity of wetland patterns in the Geomorphological Units and the breadth of the study area.

Regarding the number of samples, in applications that require image classification, the availability of labeled samples (training data) is associated with the choice that the analyst will make for extracting information from the images (ZANOTTA; ZORTEA; FERREIRA, 2019). In addition, the number of training samples available to model each class of interest, and how well these samples represent the diversity of land cover patterns in the image to be analyzed, are crucial factors for the success of supervised classification. It is well understood that the more complex the classification model being adopted, the greater the need for training samples (ZANOTTA; ZORTEA; FERREIRA, 2019).

We created 4,000 sampling points randomly, according to pre-existing limits in the inventory of the Zoobotanical Foundation of Rio Grande do Sul (FZB, 2013), considering that this inventory has consolidated information. Although there are different types of Wetlands, in this work, due to the main objective, which is to identify Potential Wetlands, only the Wetland and No Wetland classes were defined.

Samples from the No Wetland class were allocated to regions not covered by the FZB (2013) database and polygons. For this class, 4,000 sample points were also used randomly. To consolidate the samples inserted in the image classification, the databases were joined, totaling 8,000 points, to extract, later, information from each pixel of the stack of images intersected by the points, Figure 4.

Figure 4- Distribution of sampling points for Wetland and No Wetland classes, in the Central Depression (CD) and Coastal Plain (CP), Rio Grande do Sul.

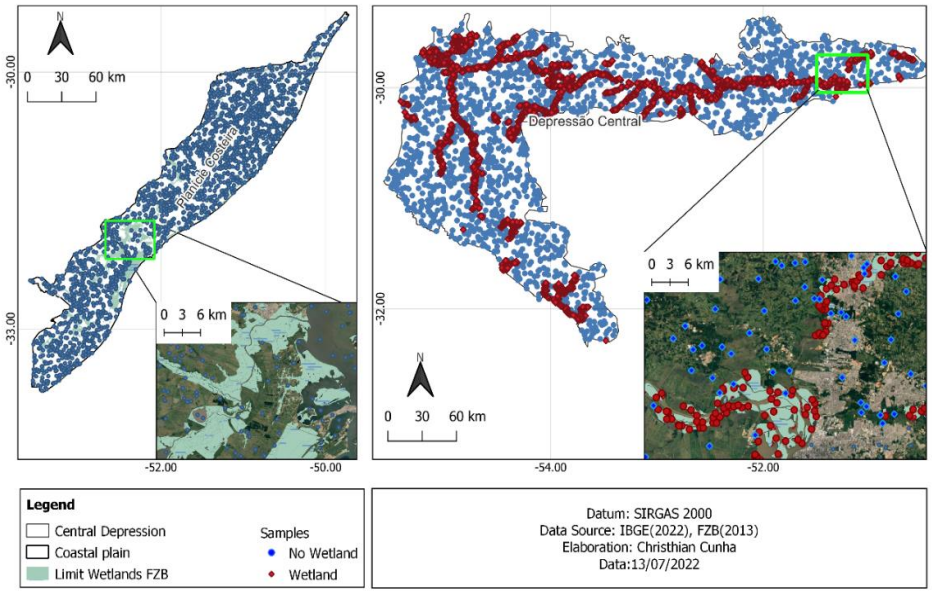

Elaboration: The authors (2023).

2.3 Image collections, different sensors, and spectral indices

Satellite images from Landsat 8 Operational Land Imager (OLI), Sentinel-1C-band SAR (C-SAR), Shuttle Radar Topography Mission (SRTM) and MODIS Evapotranspiration (MOD16A2 Version 6) sensors were selected for the period between 01/January/2015 and 31/December/2020, Table 1.

Table 1 - Datasets available in Google Earth Engine to classify PW.

Sensor	Processing	Resolution (m)	Use	Acquisition (days)
Landsat 8 OLI	Level 2 SR Tier 1	30	Surface Reflectance	8 to 16 days
Sentinel-C-SAR	Level 1 GRD	10	Backscatter intensity	5
SRTM	Level 2 Version 3	30	Elevation;slope;hillshade, aspect	-
MOD16A2	Version 6	500	Total Evapotranspiration (ET), Potential Total Evapotranspiration (PET)	8

Elaboration: The authors (2022).

From Landsat 8 (OLI), the following indices were calculated: Normalized Difference Water Index (NDWI); Modified Normalized Difference Water Index (MNDWI); Normalized Difference Vegetation Index (NDVI); Enhanced Vegetation Index (EVI); Land Surface Water Index (LSWI) used to highlight features associated with vegetation, water, and soil moisture, Table 2.

Table 2 - Spectral index Vegetation and water used in the composition of the classification.

Index	Formulation	Reference
Normalized Difference Vegetation Index	$NDVI = \frac{NIR - RED}{NIR + RED}$	Rouse et al.(1973)
Normalized Difference Water Index	$NDWI = \frac{GREN - NIR}{GREEN + NIR}$	McFeeters (1996)
Modified Normalized Difference Water Index	$MNDWI = \frac{GREN - SWIR}{GREEN + SWIR}$	Xu (2005)
Land Surface Water Index	$LSWI = \frac{NIR - SWIR}{NIR - SWIR}$	Gao (1996), Chandrasekar et al.(2010)
Enhanced Vegetation Index	$EVI = G \times (\frac{(NIR-R)}{(NIR+C1 \times R-C2 \times B+L)})$	Huete (2002)

Elaboration: The authors (2022).

Sentinel-1 imagery was used to assist in the identification of PW due to its sensitivity to herbaceous and wetland vegetation features, as well as the change from exposed soil to vegetation, wetlands, and water due to backscatter (VALENTI et al., 2020; JAMALI et al., 2021). In addition, Sentinel-1 images detect vegetation features on cloudy days or nights (PETIT et al., 2022).

To understand the importance of the elevation and slope variables, the SRTM digital elevation model (DEM), 30 m spatial resolution, was used.

The regions where the wetlands are located have different behavior and responses from the others, and thus, it was sought to verify how the processes related to evapotranspiration occur in these regions. MOD16A2 Version 6, an 8-day composite product with 500 m spatial resolution, was used for evapotranspiration. The algorithm used to collect the MOD16 data product is based on the logic of the Penman-Monteith equation, which includes daily meteorological reanalysis data inputs along with MODIS remote sensing data products, such as dynamics of vegetation properties, albedo and land cover.

Mapping approaches that use imagery and sensors that capture evapotranspiration can be useful in short-term wetland recovery assessment projects that occur during the dry season or long-term projects that compare ET rates from the dry season site to other seasons (CERON et al., 2015).

Different sensors and satellites allow significant results to be obtained to distinguish spectral behaviors that aid in the separation of distinct classes or uses. In works similar to what we propose in this paper, collections of images and different sensors have been used in wetland classification (VALENTI et al., 2020; JAMALI et al., 2021; LONG et al., 2021).

2.4 Workflow and Data Processing

Javascript language code structures in Google Earth Engine's Code Editor platform were used to acquire and digitally process the images. Advanced supervised machine learning and deep learning algorithms, such as support vector machine (SVM), k-means neighbor, random forest (RF), convolutional neural networks, and fully convolutional networks, have been successfully applied for wetland classification (HAN; DEVLIN, 2018).

The proposed mapping and supervised classification method considered data from different platforms and sensors, and made use of the pixel-based Random Forest machine learning algorithm, considering predefined classes and regions. Two mapping classes were generated: Wetlands and No Wetlands. The mapping of the PW was performed from supervised classification using Machine Learning techniques and cloud image processing using Google Earth Engine, as per the flowchart in Figure 5.

The processing began with the definition of the study area and the filtering of the images in the analysis period and region of interest. The initial proposal was to apply a single classification for the entire territory of the State of Rio Grande do Sul. However, during the development of the classification process, Google Earth Engine processing limitations (errors and time-outs) appeared, which did not allow the advance of the classification for the entire state with the adequate number of samples to obtain good results. By decreasing the number of samples, partial results showed confusion of the classifier. Areas known and consolidated as wetlands were not being mapped, or were mapped partially.

In this sense, it was chosen to perform the classification in a fragmented way by geomorphological regions. In this study, the PW classification was performed for the Central Depression and Coastal Plain Units. Limitations in large-scale image processing are pointed out by Noel et al., (2017); Valenti et al., (2020).

The data used in the classification has atmospheric, radiometric and geometric calibration and correction. Radar images were converted from decibels to obtain natural backscatter values for the VV and VH bands (VALENTI et al., 2020; JAMALI et al., 2021). On the Landsat images (OLI) a cloud mask function, and the scale and offset factor were applied. On the MOD16A2 images, the scale factor described in its properties was applied for the bands used PET and ET (USGS, 2018).

Spectral indices (NDWI, MNDWI, NDVI, EVI, LSWI, VV and VH backscatter and VV/VH ratio) used as input to the classification model were calculated, and commonly used for wetland classification due to their ability to distinguish vegetation and water characteristics from other land cover types (VALENTI et al., 2020; LONG et al., 2021).

To delineate the water bodies and to avoid overlap and confusion in the classification of wetlands, the JRC Global Surface Water Mapping Layers database was used (PEKEL et al., 2016).

Figure 5 - Flowchart of the activities for mapping the PW.

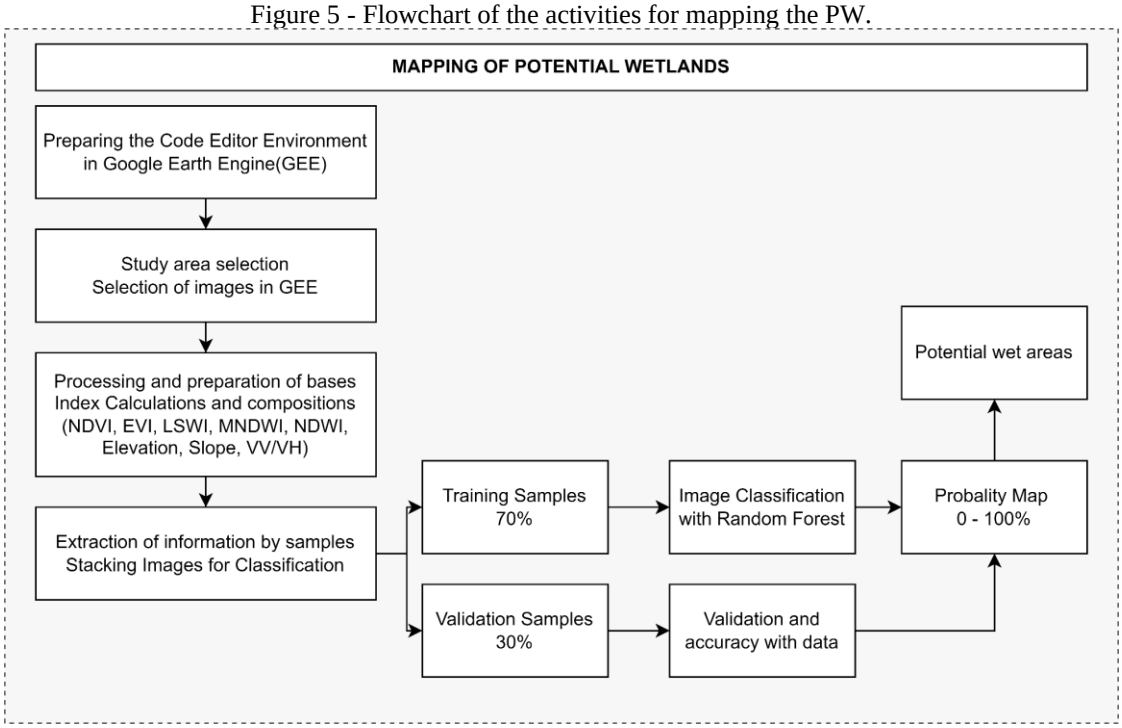

Elaboration: The authors (2022).

To identify inundated wetlands, radar data and VV and VH backscatter values and the VV/VH ratio were used. Areas of apparent water have low backscatter values due to soft surface scattering (VALENTI et al., 2020; LONG et al., 2021). Flooded wetlands have high backscattering values due to double-bounce scattering (AHMAD et al., 2020; VALENTI et al., 2020). The VV/VH ratio is particularly useful for wetland classification due to sensitivity to soil moisture and correction for terrain effects (VALENTI et al., 2020; LONG et al., 2021).

Random Forest (RF), a non-parametric machine learning algorithm that creates decision trees (DT) based on training data and spectral bands organized into a stack of input images, was used (JAMALI et al., 2020; VALENTI et al., 2020). The Random-based classification approach combines classifier trees generated using a random training sample data set. Each tree provides a vote for the class in which an input vector should be located (BREIMAN 2001).

When a sample is entered into the RF model, each decision tree performs a separate evaluation to determine the category to which the sample should belong, and the category that is selected most often is considered the category of the sample. The RF method can effectively reduce the uncertainty of a specific algorithm and improve the accuracy of classification. The information dimension of RF processing is larger and more complex than that of other classification algorithms (HU et al., 2017).

The literature indicates that RF outperforms other classifiers, including Naive Bayes (NB), Classification and Regression Tree (CART), and Support Vector Machine (SVM), in wetland mapping. In their study, Gxokwe, Dube and Mazvimavi (2022) evaluated various classifiers and found that RF yielded the most satisfactory results, achieving the following accuracies: RF (80.55%), NB (25%), SVM (66.60%), and CART (62.30%). Amani (2018) and Amani et al. (2019) used the RF algorithm based on studies where the RF algorithm was superior to other classifiers commonly used for wetland mapping. In Mahdianpari et al., (2020) research, the RF yields more accurate results than CART and Minimum Distance (MD) for large-scale wetland monitoring.

The RF pixel-by-pixel method was used because of the high processing capacity of the GEE and because it produces satisfactory results that are not significantly different from object-based approaches in wetlands (VALENTI et al., 2020; JAMALI et al., 2020; LONG et al., 2021; HU et al., 2017).

This method is often used in wetland mapping because it can handle datasets from multiple sources,

has few observations, and is not normally distributed, remaining insensitive to overfitting and noise (VALENTI et al., 2020; JAMALI et al., 2020; LONG et al., 2021).

In the classification process, the samples were randomized, and divided into training and validation samples, in the proportion of 70% for classifier training samples and 30% for accuracy testing. The trained RF classifier was applied to the database containing the different image collections, spectral bands and sensors to create a PW classification. An RF classifier with 500 trees and the default GEE settings was used. The RF uses decision trees to classify, selecting the class with the most votes among all trees. In this work, the output mode is assigned the variable "PROBABILITY" which indicates the probability that the classification is correct, with values ranging from 0 to 100%.

To evaluate the Wetlands mapping for the CP and CD geomorphological units, we performed the overlay of the FZB (2013) database over the supervised classification obtained for the WP.

Classification accuracy was performed based on the training samples and a consistency evaluation based on the FZB Wetlands mapping (2013). The accuracy evaluation was performed with randomly distributed verification samples, and used confusion matrices, producer accuracy (sample fractions of pixels of each class correctly assigned to their classes by the classifiers, associated with omission error) and user accuracy (estimates of the fractions of mapping pixels, for each class, correctly classified, associated with commission error) according to Hu et al. (2017); Valenti et al., (2020); Long et al., (2021).

3 RESULTS AND DISCUSSION

3.1 Spectral response of bands and indices per class

The boxplot analysis, Figure 6 shows the spectral response and index values for the Wetlands and No Wetlands samples for the Central Depression (CD) and Coastal Plain (CP) geomorphological units.

In relation to the vegetation (NDVI and EVI) and water (LSWI, NDWI and MNDWI) indices, as well as the bands (VV, VH, Blue, Green, Nir, Red, Swir1, Swir2, Slope, Elevation, Temperature, Aspect, ET and PET) it is possible to identify a similar behavior of the spectral responses for the classes analyzed in the two units (CP and CD). The classes tend to present maximum and minimum values in close proportions and distributions.

The NDVI analysis allows us to observe that the Wetlands samples show higher maximum and median values when compared to the No Wetlands samples in CP and CD. The maximum NDVI values are higher and distinct between the classes, as the Wetlands show higher concentrations of vegetation than the No Wetlands in the geomorphological regions.

For EVI this behavior was distinct, and it was not possible to identify a pattern in the maximum values and medians in the two regions as in the case of NDVI and other indices. It is noted that the medians of the CD samples are very close between the Wetlands and No Wetlands classes, differently from what is identified in the CP.

Long et al., (2021), in a similar mapping, used spectral indices with good separability between classes. When considering a larger number of classes, EVI, for example, showed spectral responses providing a better degree of discrimination, however distinguishing wetland vegetation types using NDVI and NDWI was difficult.

The NDWI and MNDWI indices highlight water bodies and allow monitoring of dynamic changes in wetlands. Water has a direct impact on wetland ecosystem dynamics, and hydrological variables such as evapotranspiration, flood duration, flow velocity, and flow variability, and can be used to assess wetland health (CERON et al., 2015). In addition, understanding the seasonality of streams in relation to their permanence and hydrological regime is important for this ecosystem (ASHOK et al., 2021).

In this context, work done for monitoring wetlands has shown the significant perception of change in terms of pixel range with the presence of water and changing locations in terms of seasonality and resilience (ASHOK et al., 2021; VALENTI et al., 2021, HALABISKY et al., 2022). The box plot outliers concerning the wetland samples for the two units (CD and CP) are estimated to be the presence of water sheet or moisture in periods of flooding pulses (Figure 6).

 DOI: http://dx.doi.org/10.14393/rbcv75n0a-69753

Figure 6 - Spectral and index values of the randomly selected samples for the Central Depression (CD) and Coastal Plain (CP).

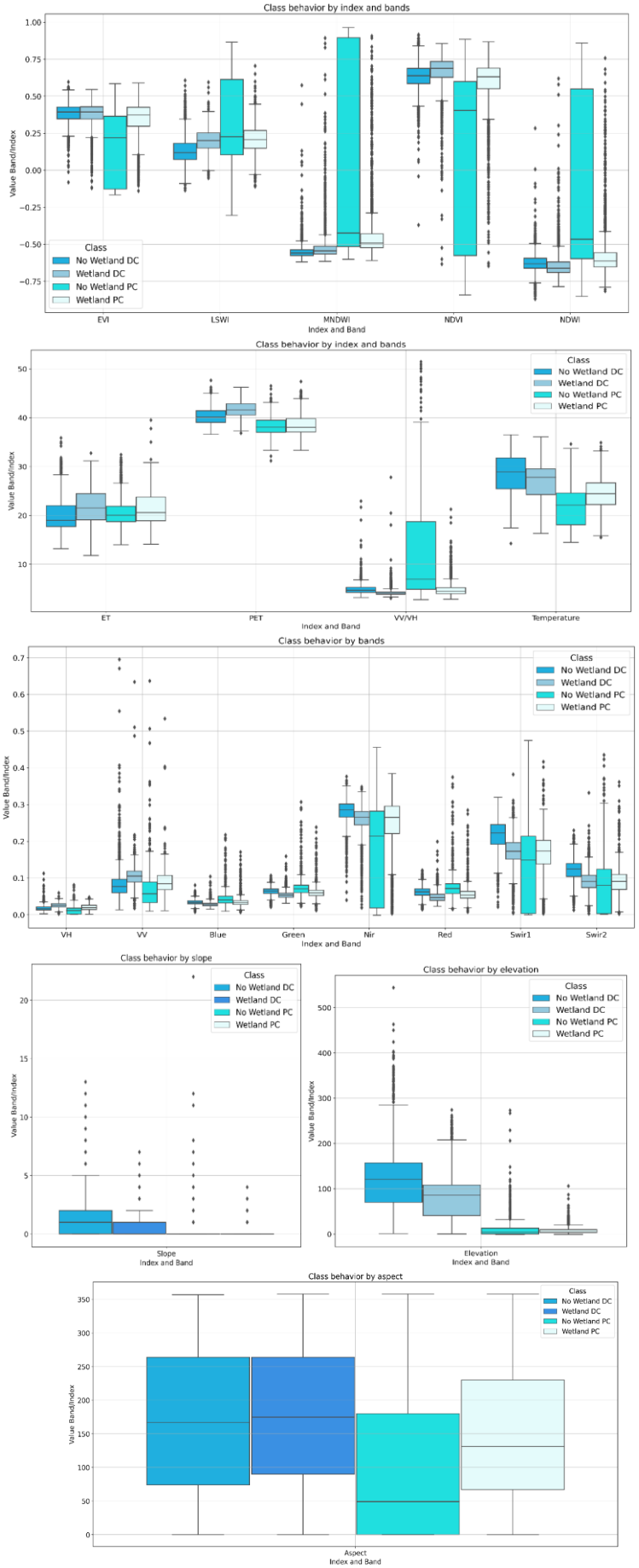

Elaboration: The authors (2023).

Considering climatological aspects, wetland regions, due to the presence of soil moisture, flood pulses, and water sheet, tend to have lower temperatures than their surroundings. In addition, wetlands have a cooling effect in tropical regions (WU et al., 2021).

Wetlands tend to have higher volumes for evapotranspiration and potential evapotranspiration. In addition, evapotranspiration is a reliable indicator of wetland health (CERON et al., 2015). Expected behaviors for temperature, ET and PET, described in Ceron et al., (2015); Moreira et al., (2019), were observed in our results for the two mapped geomorphological units. Although, they have distinct maximum values, wetlands show lower temperatures than the other No Wetlands regions, while the results for ET and PET are higher.

The spectral responses of the indices and bands for the CD and CP regions are distinct due to the different land cover, land use and land cover compositions in these geomorphological units. In Figure 8 and Figure 10 it is observed that the CP unit presents a greater extension of water bodies, for example. However, even with distinct land uses, it was possible to observe patterns in the spectral responses of the Wetlands and No Wetlands.

Another aspect verified in the graphical analysis is that all 5 indices analyzed for CP, have significant interquartile range. This amplitude may be due to the heterogeneity found in the soil cover of the region.

The VV/VH ratio showed different results for the CP and CD units. Such divergences may have occurred due to the effects of terrain and soil moisture. The VV/VH ratio is particularly useful for wetland classification because of its sensitivity to soil moisture, and it also corrects for terrain effects (VALENTI et al., 2020).

In the analysis of elevation, slope, and aspect of the samples in the image classification, the results were similar in the two units. The wetlands occur in regions of lower elevation and lower slope in both geomorphological units. In a study conducted for wetlands in Canada, slope and elevation had a strong influence on classification (VALENTI et al., 2020).

3.2 Mapping Evaluation

The results of the geomorphological unit's classification (Figure 8, 9, 10 and Figure 11) show that the pixels classified by the RF algorithm with the highest probability of being PW overlap the database of the FZB. The classification differentiated Wetlands and No Wetlands in unsampled regions (Figure 7). It is estimated, however, that some areas may have been misclassified due to the limitations of the pixel-by-pixel classification method, as well as by the results pointed out in the statistical analyses presented in Table 3.

Pixels near or within the FZB polygons were also more likely to have been correctly classified as Potential Wetlands (Figure 8 and Figure 10).

A Table 3 presents the areas of the existing Wetlands in each geomorphological unit (CD and CP), against the result of the total area obtained after classification. It can be seen that for both regions, the area classified for the PW is larger than the reference database. For the CP, the percentage difference was 22% between the area mapped, and the area classified as PW, as well as for the CD, the difference was 24%.

In this context, it can be said that, on average, in the two regions, more than 20% of the existing areas are PW that are not mapped in existing inventories.

Table 3 - Statistical Analysis for Wetlands and No Wetlands, in the Central Depression (CD) and Coastal Plain (CP).

Area km² Central Depression				**Area km² Coastal Plain**			
FZB Area	Classified Area	Difference	Difference %	FZB Area	Classified Area	Difference	Difference %
1452.33	1923.10	470.77	24%	3495.2	4453.85	958.65	22%

Elaboration: The authors (2023).

Figure 7 - PW in relation to the FZB Wetlands database (black outline) in the Central Depression (CD).

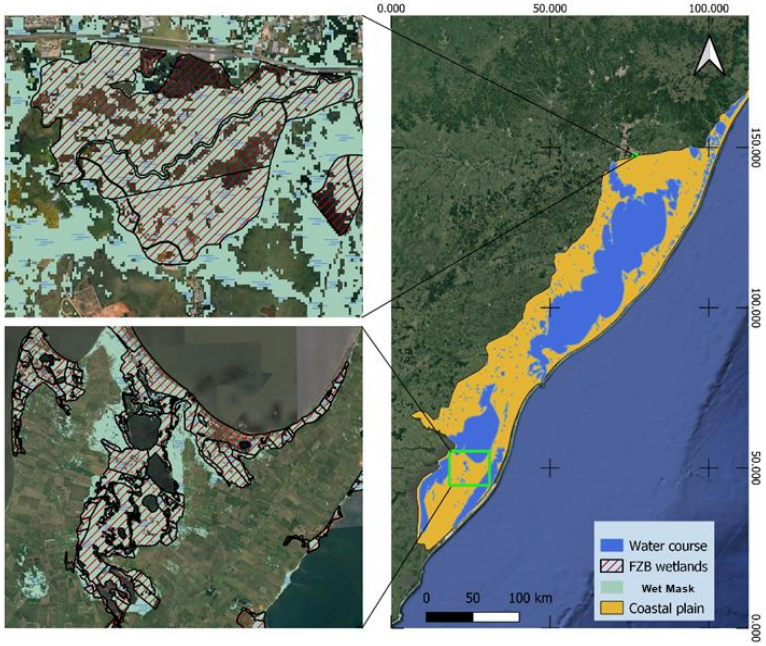

Elaboration: The Authors (2023).

Figure 8 - PW (pink) in relation to the FZB Wetlands database (black outline) in the Central Depression (CD).

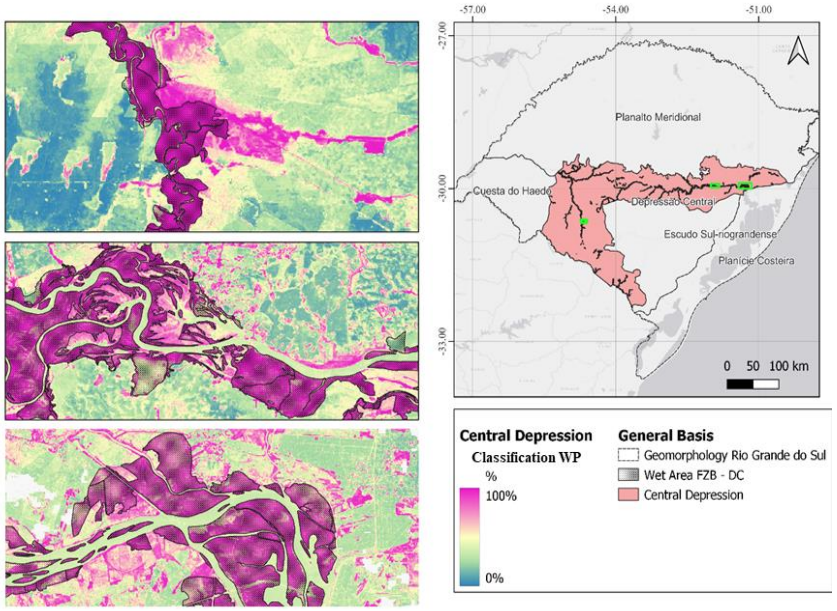

Elaboration: The Authors (2023).

Our study sought to understand and define the spectral responses, topographic, geomorphological and hydrological characteristics to define regions that present similarities and can be classified as PW. In this sense, it is also observed that some pixels, beyond the boundaries of existing polygons and already classified as wetlands, also presented high probability of being wetlands according to the classification (above 80%, see Table 3).

In studies using similar methodologies, errors in wetlands mapping were also observed. In this case, the extent of Potential Wetlands was sometimes overestimated on slopes or, conversely, underestimated on small alluvial ridges or road embankments (RAPINEL et al., 2019).

The analysis of the importance of the variables in the classification process (Figure 9), shows that the bands referring to Elevation, Temperature, VH, VV/VH, ET, NIR, VV, BLUE, LSWI, PET, and SWIR2 presented, in this order, greater importance for the RF classifier.

Based on the spectral responses of the bands and indices identified as of greatest importance during image classification, it stands out that elevation and temperature had the greatest influence on the classifier, as well as presenting strongly distinct spectral responses for the Wetlands and No Wetlands classes.

According to Breiman (2001) variable importance analysis allows identifying why a certain variable seems important, and how the insertion of others may help or hinder image classification once inserted. In image classification, the analysis of the importance of variables also illustrates the relevance of the data aiming for higher overall classification accuracy in the proposed model (KELLEY; PITCHER; BACON, 2018). In this case, these bands would be the variables that most influence the classifier to distinguish Wetlands from No Wetlands.

Stream delineation databases from the JRC Global Surface Water Mapping Layers collection (PEKEL et al., 2016) were used to aid wetland classification. However, this information did not carry weight in the RF decision-making (ocurrence e max extent bands).

Figure 9 - Importance of variables for Random Forest classification, Central Depression (CD).

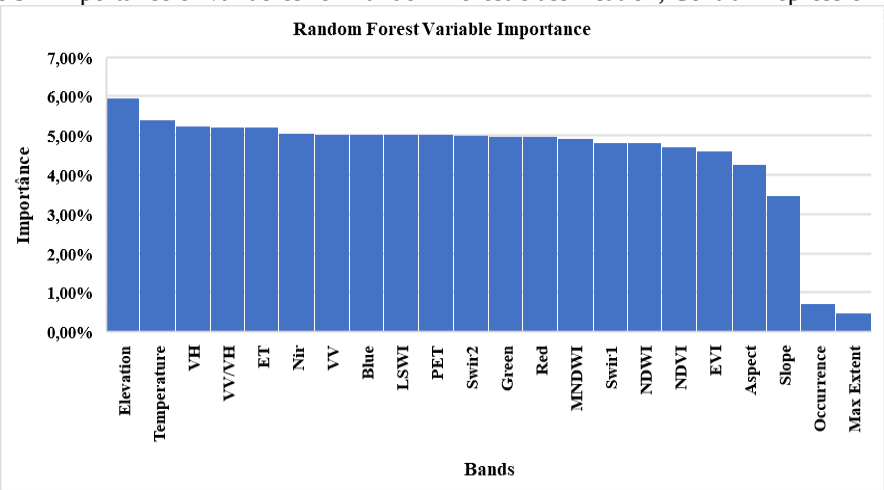

Elaboration: The Authors (2023).

For the Coastal Plain (CP) the results show a similar behavior to the PW of the Central Depression (CD) in terms of spectral responses and importance of the variables in the classifier. Furthermore, as mentioned earlier, the classification covers other areas beyond the FZB inventory, identifying, from the spectral response, other regions that can be framed as PW and that have not yet been mapped in existing inventories.

Although the importance of the variables alternated between the units, our results allow us to identify areas that fit as PW from the spectral signatures and reinforce that the methodology employed was satisfactory. Rapinel et al., (2019); Valenti et al., (2020); Ashok et al., (2021) used different image and sensor bases for classification and were also able to separate classes from spectral and topographic signatures.

Figure 10 - PW (pink) in relation to the wetland's database (black outline) of the FZB, Coastal Plain (CP) region.

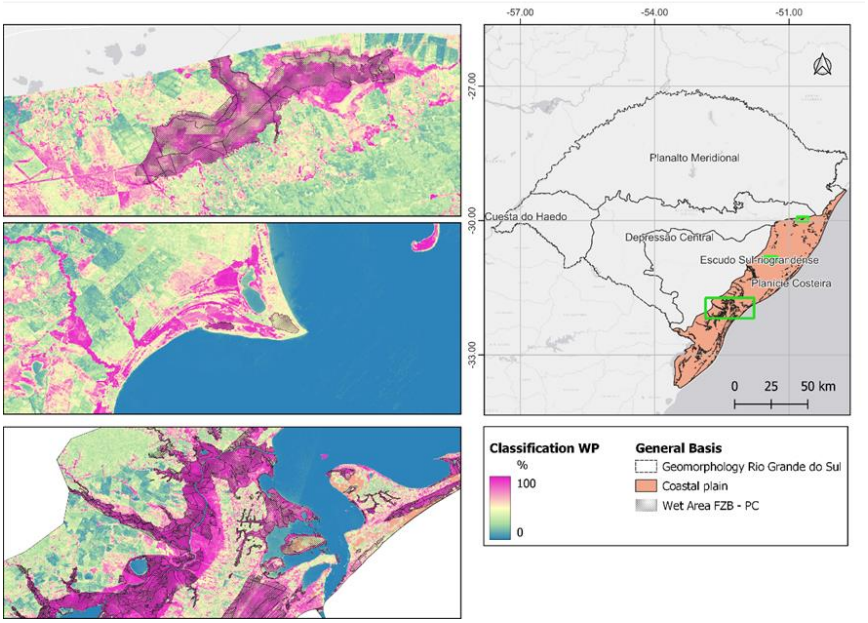

Elaboration: The Authors (2023).

Comparing the results between the Central Depression units (Figure 9) and Coastal Plain (Figure 11) shows that the bands corresponding to Elevation, Temperature, VH, VV, BLUE, VV/VH and LSWI are the most important variables for the RF classifier.

Figure 11 - Importance of variables for Random Forest classification, Coastal Plain (CP).

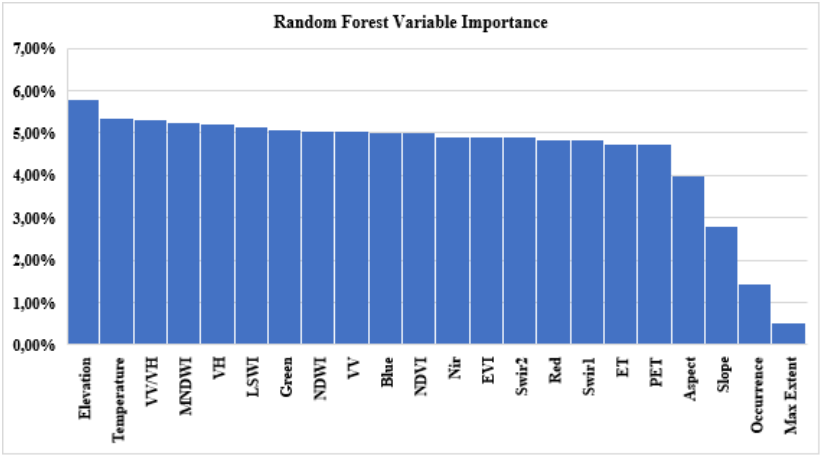

Elaboration: The Authors (2023).

Unlike what was obtained for the Central Depression, the variables corresponding to ET and PET do not have similar importance for the Coastal Plain, which may be associated with the differences in land use and occupation in the two geomorphological units.

On the other hand, PW are estimated to have higher evapotranspiration potential than the other classes that were grouped as No Wetlands (CERON et al., 2015). In this sense, it was expected that the spectral responses for ET and PET would be among the most important values for the Random Forest classifier.

The similarities found in the two mapped units allow us to affirm that the spectral responses are determining variables for the classification of PW and the use of different sensors and satellites allows the classification algorithm to establish distinct thresholds and, based on this, to more accurately determine the class associated with each sample.

In wetland inventories and mapping using different sensors (CERON et al., 2019; RAPINEL et al.,

2019; VALENTI et al., 2020; ASHOK et al., 2021; LONG et al., 2021; WU et al., 2021) besides obtaining distinct spectral responses for the classes and allowing separation from thresholds, more accurate results were obtained.

3.3 Accuracy of the RF classification

The proposed methodology, based on the data set for the Central Depression and Coastal Plain units, achieved Overall Accuracy of 89% and 88%, respectively (Table 4).

Consumer accuracy averaged 83% for No Wetland and 93% for Wetland (PW) for the Central Depression unit. For producer accuracy, the values obtained were 87% and 91% for No Wetland and Wetland. For the Coastal Plain unit, the overall accuracy was 88%, while the Producer and Consumer accuracy was 89% and 81% for No Wetland and 88% and 94% for Wetland (PW).

As to the Kappa index, both units averaged results between 75% and 77%, suggesting that the classifications were in generally high agreement with the validation data, even considering the random agreement between the datasets.

Based on the results of accuracy and Kappa index, it is understood that the methodology proposed for the classification of Potential Wetlands produced results consistent with previous inventories already conducted in the region, as in the case of the study produced by FZB (2013).

Table 4 - Statistical Analysis for Wetlands and No Wetlands in the geomorphological units

Accuracy Classification Central Depression				
Class	**Consumer Accuracy**	**Producer Accuracy**	**Overall validation accuracy**	**Kappa Coefficient**
In the Wetland	83%	87%	-	-
Wetland	93%	91%	-	-
General	-	-	89%	77%
Accuracy Classification of Coastal Plain				
Class	**Consumer Accuracy**	**Producer Accuracy**	**Overall validation accuracy**	**Kappa Coefficient**
In the Wetland	89%	81%	-	-
Wetland	88%	94%	-	-
General	-	-	88%	75%

Elaboration: The Authors (2023).

3.4 Mapping limitations

According to Valenti et al., (2020), GEE has a high potential for global processing and analysis. However, there are limitations in terms of user memory and computational time, which may pose problems in the development of in-depth methodologies or large-scale studies, as reported in the mapping of wetlands with similar methodology.

The methodological proposal for the classification of potential wetlands based on the geomorphological units of the State of Rio Grande do Sul aims to understand the spectral behavior and define mapping patterns. However, when developing the classification process, there were processing limitations (errors and timeouts) in Google Earth Engine.

When performing the classification for the entire area of the State of Rio Grande do Sul using 8000 samples, the processing capacity was exceeded due to the size of the area, the number of bands, and the complexity of the analysis. To make the classification of AUs feasible, different sampling methods and sample quantities were tested to define wetlands and non-wetlands. The approach with the best results was a fragmented classification into geomorphological regions using 8000 samples to overcome the limitations of large scale processing. These limitations have also been pointed out by Noel et al. (2017); Valenti et al. (2020).

4 CONCLUSIONS

The approach to classify Potential wetlands had as reference different methodological proposals that

suggest the use of remote sensing data and techniques, digital image processing and image classifications from machine learning for large areas using Google Earth Engine (GEE).

In this sense, we developed the mapping for two geomorphological units of the state of Rio Grande do Sul, to identify potential wetlands. The separate classification of the units Central Depression and Coastal Plain allowed the results to be more accurate and consistent with the reality found in previous mappings and consolidated by competent environmental agencies.

Potential wetlands were mapped with a global accuracy higher than 88% and consumer and producer accuracies higher than 85% in the Coastal Plain and Central Depression. Such results allow concluding that the proposed methodology allows the identification, from spectral signatures, and pixel-by-pixel supervised classification of PW using different image collections and sensor systems.

Our results indicate that it is necessary to re-evaluate and update the existing inventories, as wetlands may be larger than the current maps represent.

The use of passive optical data and radar images optimized the results obtained, as did the use of phenology and water indices, as well as temperature, evapotranspiration, elevation, and slope data that were considered important variables and influenced the classification of the images.

Finally, it is understood that the mapping of PW can assist in the identification and enlargement of sites that have not been correctly classified in the existing inventories. However, field data collection and photographic records at sites that have been identified as potential wetlands can be gauged to result in a more accurate and updated inventory.

Acknowledgments

This study was financed in part by the Coordination for the Improvement of Higher Education Personnel – Brazil (CAPES) – Financing Code 001, by the Rio Grande do Sul State Research Support Foundation (FAPERGS) via the Gaúcho Researcher Program, notice 07/2021 and by Research Productivity Grant from the National Council for Scientific and Technological Development (CNPq).

Author's contributions

The authors Christhian Santana Cunha, Laurindo Antonio Guasselli, Tássia Fraga Belloli and Carina Cristiane Korb jointly defined the conceptualization and methodology used. These were responsible for data curation, formal analysis, investigation, validation, visualization, and writing-review and editing.

Conflicts of Interest

The authors have no conflicts of interest to declare.

References

AHMAD, S. K.; HOSSAIN F.; ELDARDIRY, H.; PAVELSKY, T. M. A Fusion Approach for Water Area Classification Using Visible, Near Infrared and Synthetic Aperture Radar for South Asian Conditions. **Ieee Transactions On Geoscience And Remote Sensing**, [S.L.], v. 58, n. 4, p. 2471-2480, abr. 2020. Institute of Electrical and Electronics Engineers (IEEE). DOI: 10.1109/tgrs.2019.2950705.

ALIKHANI, S.; NUMMI, P.; OJALA, A. Urban Wetlands: a review on ecological and cultural values. **Water**, [S.L.], v. 13, n. 22, p. 3301, 22 nov. 2021. MDPI AG. DOI: 10.3390/w13223301.

AMANI, M. Wetland inventory system for NL using satellite data (what has been done and what is next step). In: **Proc. Real Time Water Qual. Monit. Workshop**. 2018. DOI: 10.13140/RG.2.2.23031.27044.

AMANI, M; MAHDAVI, S.; AFSHAR, M.; BRISCO, B.; HUANG, W.; MIRZADEH, S. M. J.; WHITE, L.; BANKS, S.; MONTGOMERY, J.; HOPKINSON, C. Canadian Wetland Inventory using Google Earth Engine: the first map and preliminary results. **Remote Sensing**, [S.L.], v. 11, n. 7, p. 842, 8 abr. 2019.

MDPI AG. DOI: 10.3390/rs11070842.

ASHOK, A.; RANI, H. P.; JAYAKUMAR, K. V. Monitoring of dynamic wetland changes using NDVI and NDWI based landsat imagery. **Remote Sensing Applications: Society and Environment**, v. 23, p. 100547, 2021. DOI: 10.1016/j.rsase.2021.100547.

ASOKAN, A.; ANITHA, J. Change detection techniques for remote sensing applications: A survey. **Earth Science Informatics**, v. 12, p. 143-160, 2019. DOI: 10.1007/s12145-019-00380-5.

AYANLADE, A.; PROSKE, U. Assessing Wetland Degradation and Loss of Ecosystem Services in the Niger Delta, Nigeria. **Marine and Freshwater Research,** v. 67, n. 6, p. 828-836, 2015. DOI: 10.1071/MF15066.

BAN, Y.; YOUSIF, O. Change Detection Techniques: A Review. In: Ban, Y. (eds) **Multitemporal Remote Sensing. Remote Sensing and Digital Image Processing**, vol 20, p. 19-43, 2016. Springer, Cham. DOI: 10.1007/978-3-319-47037-5_2.

BERTHIER, L.; GUZMOVA, L.; LAROCHE, B.; LEHMANN, S.; SQUIVIDENT, H.; MARTIN, M.; CHENU, J.; THIRY, E.; LEMERCIER, B.; BARDY, M.; MÉROT, P.; WALTER, C. Spatial prediction of potential wetlands at the French national scale based on hydroecoregions stratification and inference modelling. In: **EGU General Assembly Conference Abstracts**. 2014. p. 12780.

BOURGEAU-CHAVEZ, L.; ENDRES, S.; BATTAGLIA, M.; MILLER, M.; BANDA, E.; LAUBACH, Z.; HIGMAN, P.; CHOW-FRASER, P.; MARCACCIO, J. Development of a Bi-National Great Lakes Coastal Wetland and Land Use Map Using Three-Season PALSAR and Landsat Imagery. **Remote Sensing**, [S.L.], v. 7, n. 7, p. 8655-8682, 9 jul. 2015. MDPI AG. DOI:10.3390/rs70708655.

BREIMAN, L. Random forests. **Machine learning**, v. 45, p. 5-32, 2001.

BRINSON, M. M.; CHRISTIAN, R. R. Assessing functions of wetlands and the need for reference. **Biologia Ambientale**, v. 24, n. 1, p. 307-318, 2010.

BRINSON, M. M. A hydrogeomorphic classification for wetlands, reference wetlands, and functional indices. Vicksburg: **US Army Engineers Waterways Experiment Station**, 1993. 175p.

CERON, C.; MELESSE, A.; PRICE, R.; DESSU, S.; KANDEL, H. Operational Actual Wetland Evapotranspiration Estimation for South Florida Using MODIS Imagery. **Remote Sensing**, [S.L.], v. 7, n. 4, p. 3613-3632, 26 mar. 2015. MDPI AG. DOI: 10.3390/rs70403613.

CHANDRASEKAR, K.; SAI, M. V. R. S; ROY, P. S.; DWEVEDI, R. S. Land Surface Water Index (LSWI) response to rainfall and NDVI using the MODIS Vegetation Index product. **International Journal Of Remote Sensing**, [S.L.], v. 31, n. 15, p. 3987-4005, 10 ago. 2010. Informa UK Limited. DOI: 10.1080/01431160802575653.

DASILVA, M. D.; BRUCE, D; HESP, P. A.; SILVA, G. M. da. A New Application of the Disturbance Index for Fire Severity in Coastal Dunes. **Remote Sensing**, [S.L.], v. 13, n. 23, p. 4739, 23 nov. 2021. MDPI AG.. DOI: 10.3390/rs13234739.

DURAND, P.; GASCUEL-ODOUX, C.; KAO, C.; MEROT, P. Une typologie hydrologique des petites zones humides ripariennes. **Etude et gestion des sols**, v. 7, n. 3, p. 207-218, 2000.

FARR, T. G.; ROSEN, P. A.; CARO, E.; CRIPPEN, R.; DUREN, R.; HENSLEY, S.; KOBRICK, M.; PALLER, M., RODRIGUEZ, E., ROTH, L., SEAL, D., SHAFFER, S., SHIMADA, J., UMLAND, J., WERNER, M; OSKIN, M.; BURBANK, D.; ALSDORF, D. E. The shuttle radar topography mission. **Reviews of geophysics**, v. 45, n. 2, 2007.DOI: 10.1029/2005RG000183.

FRANKLIN, S. E.; SKERIES, E. M.; STEFANUK, M. A.; AHMED, O. S. Wetland classification using Radarsat-2 SAR quad-polarization and Landsat-8 OLI spectral response data: A case study in the Hudson Bay Lowlands Ecoregion. **International Journal of Remote Sensing**, v. 39, n. 6, p. 1615-1627, 2018. DOI: 10.1080/01431161.2017.1410295

GALLANT, A. The Challenges of Remote Monitoring of Wetlands. **Remote Sensing**, [S.L.], v. 7, n. 8, p. 10938-10950, 24 ago. 2015. MDPI AG. DOI: 10.3390/rs70810938.

GAO, B. C. Normalized difference water index for remote sensing of vegetation liquid water from space. In: **Imaging spectrometry**. SPIE, 1995. p. 225-236.

GOKCE, D. **Wetlands Management: Assessing Risk and Sustainable Solutions**. BoD–Books on Demand, 2019. DOI: 10.5772/intechopen.76596

GOMES, C. S.; JÚNIOR, A. P. M. Sistemas de classificação de áreas úmidas no Brasil e no mundo: panorama atual e importância de critérios hidrogeomorfológicos. **Geo UERJ**, n. 33, p. 34519, 2018. DOI: 10.12957/geouerj.2018.34519.

GORELICK, N.; HANCHER, M.; DIXON, M.; ILYUSHCHENKO, S.; THAU, D.; MOORE, R. Google Earth Engine: Planetary-scale geospatial analysis for everyone. **Remote sensing of Environment**, v. 202, p. 18-27, 2017. DOI: 10.1016/j.rse.2017.06.031.

GUADAGNIN, D. L.; MALTCHIK, L. Habitat and landscape factors associated with neotropical waterbird occurrence and richness in wetland fragments. **Biodiversity And Conservation**, [S.L.], v. 16, n. 4, p. 1231-1244, 27 out. 2006. Springer Science and Business Media LLC. DOI: 10.1007/s10531-006-9127-5.

GUADAGNIN, D. L; MALTCHIK, L.; FONSECA, C. R. Species–area relationship of Neotropical waterbird assemblages in remnant wetlands: looking at the mechanisms. **Diversity And Distributions**, [S.L.], v. 15, n. 2, p. 319-327, 9 fev. 2009. Wiley. DOI: 10.1111/j.1472-4642.2008.00533.x

GUASSELLI, L. A.; SIMIONI, J. P. D.; LAURENT, F. Mapeamento e classificação de áreas úmidas usando Topographic Wetness Index (TWI) a partir de modelos digitais de elevação, na bacia hidrográfica do Rio Gravataí: Rio Grande do Sul, Brasil. **Revista Brasileira de Geomorfologia. Vol. 21, n. 3 (jul./set. 2020), p. 639-659**, 2020. DOI: 10.20502/rbg.v21i3.1714

GXOKWE, S.; DUBE, T.; MAZVIMAVI, D. Leveraging Google Earth Engine platform to characterize and map small seasonal wetlands in the semi-arid environments of South Africa. **Science Of The Total Environment**, [S.L.], v. 803, p. 150139, jan. 2022. Elsevier BV. DOI: 10.1016/j.scitotenv.2021.150139.

HALABISKY, M. Improved wetland identification for conservation and regulatory priorities. **University of Washington,** 2019.

HALABISKY, M.; MILLER, D.; STERWART, A. J.; LORIGAN, D.; BRASEL, T.; MOSKAL, L. The Wetland Intrinsic Potential tool: Mapping wetland intrinsic potential through machine learning of multi-scale remote sensing proxies of wetland indicators. **EGUsphere**, p. 1-19, 2022. DOI: 10.5194/egusphere-2022-665.

HAN, X.; PAN, J.; DEVLIN, A. T. Remote sensing study of wetlands in the Pearl River Delta during 1995–2015 with the support vector machine method. **Frontiers Of Earth Science**, [S.L.], v. 12, n. 3, p. 521-531, 30 out. 2017. Springer Science and Business Media LLC. DOI: 10.1007/s11707-017-0672-x.

HIRD, J.; DELANCEY, E.; MCDERMID, G.; KARIYEVA, J. Google Earth Engine, Open-Access Satellite Data, and Machine Learning in Support of Large-Area Probabilistic Wetland Mapping. **Remote Sensing**, [S.L.], v. 9, n. 12, p. 1315, 14 dez. 2017. MDPI AG. DOI: 10.3390/rs9121315.

HU, S.; NIU, Z.; CHEN, Y.; LI, L.; ZHANG, H. Global wetlands: potential distribution, wetland loss, and status. **Science Of The Total Environment**, [S.L.], v. 586, p. 319-327, maio 2017. Elsevier BV. DOI:10.1016/j.scitotenv.2017.02.001.

HUANG, W.; DEVRIES, B.; HUANG, C.; JONES, J.; LANG, M.; CREED,I. Automated extraction of inland surface water extent from Sentinel-1 data. In: **2017 IEEE International Geoscience and Remote Sensing Symposium (IGARSS)**. IEEE, 2017. p. 2259-2262. DOI: 10.1109/IGARSS.2017.8127439.

HUETE, A.; DIDAN, K.; MIURA, T.; RODRIGUEZ, E. P.; GAO, X.; FERREIRA, L. G. Overview of the radiometric and biophysical performance of the MODIS vegetation indices. **Remote Sensing Of Environment**, [S.L.], v. 83, n. 1-2, p. 195-213, nov. 2002. Elsevier BV. DOI: 10.1016/s0034-4257(02)00096-2.

JAMALI, A.; MAHDIANPARI, M.; BRISCO, B.; GRANGER, J.; MOHAMMADI, F.; SALEHI, B. Deep Forest classifier for wetland mapping using the combination of Sentinel-1 and Sentinel-2 data. **GIScience &amp Remote Sensing**, UK, v. 58, n. 7, p. 1072–1089, set. 2021. DOI: 10.1080/15481603.2021.1965399.

KAPLAN, G.; AVDAN, U. Evaluating the utilization of the red edge and radar bands from sentinel sensors for wetland classification. **Catena**, [S.L.], v. 178, p. 109-119, jul. 2019. Elsevier BV. DOI:

10.1016/j.catena.2019.03.011.

KELLEY, L. C.; PITCHER, L.; BACON, C. 2018. Using Google Earth Engine to Map Complex Shade-Grown Coffee Landscapes in Northern Nicaragua. **Remote Sensing**, [S.L.], v. 10, n. 6, p. 952, 14 jun. 2018. MDPI AG. DOI: 10.3390/rs10060952.

LONG, X.; X. LI; H. LIN; M. ZHANG. Mapping the vegetation distribution and dynamics of a wetland using adaptive-stacking and Google Earth Engine based on multi-source remote sensing data. **International Journal of Applied Earth Observation and Geoinformation**, v. 102, p. 102453, out. 2021. Elsevier BV. DOI: 10.1016/j.jag.2021.102453.

MABWOGA, S. O.; THUKRAL, A. K. Characterization of change in the Harike wetland, a Ramsar site in India, using landsat satellite data. **SpringerPlus**, v. 3, n. 1, p. 1-11, 2014. DOI: 10.1186/2193-1801-3-576.

MAHDIANPARI, M.; JAFARZADEH, H.; GRANGER, J. E.; MOHAMMADIMANESH, F.; BRISCO, B.; SALEHI, B.; HOMAYOUNI, S.; WENG, Q. A large-scale change monitoring of wetlands using time series Landsat imagery on Google Earth Engine: a case study in newfoundland. **Giscience & Remote Sensing**, [S.L.], v. 57, n. 8, p. 1102-1124, 16 nov. 2020. Informa UK Limited. DOI: 10.1080/15481603.2020.1846948.

MAHDIANPARI, M.; SALEHI, B.; MOHAMMADIMANESH, F.; BRISCO, B.; HOMAYOUNI, S.; GILL, E.; DELANCEY, E. R.; BOURGEAU-CHAVEZ, L. Big Data for a Big Country: the first generation of canadian wetland inventory map at a spatial resolution of 10-m using sentinel-1 and sentinel-2 data on the google earth engine cloud computing platform. **Canadian Journal Of Remote Sensing**, [S.L.], v. 46, n. 1, p. 15-33, 2 jan. 2020. Informa UK Limited. DOI: 10.1080/07038992.2019.1711366.

MAHDIANPARI, M.; SALEHI, B.; MOHAMMADIMANESH, F.; HOMAYOUNI, S.; GILL, E. The First Wetland Inventory Map of Newfoundland at a Spatial Resolution of 10 m Using Sentinel-1 and Sentinel-2 Data on the Google Earth Engine Cloud Computing Platform. **Remote Sensing**, [S.L.], v. 11, n. 1, p. 43, 28 dez. 2018. MDPI AG. DOI: 10.3390/rs11010043.

MAO, D.; WANG, Z.; DU, B.; LI, Lin; TIAN, Y.; JIA, M.; ZENG, Y.; SONG, K.; JIANG, M.; WANG, Y. National wetland mapping in China: a new product resulting from object-based and hierarchical classification of landsat 8 oli images. **Isprs Journal Of Photogrammetry And Remote Sensing**, [S.L.], v. 164, p. 11-25, jun. 2020. Elsevier BV. DOI: 10.1016/j.isprsjprs.2020.03.020.

MAXA, M.; BOLSTAD, P. Mapping northern wetlands with high resolution satellite images and LiDAR. **Wetlands**, v. 29, p. 248-260, 2009. DOI: https://doi.org/10.1672/08-91.1

MCCARTHY, M. J.; MERTON, E. J.; MULLER-KARGER, F. E. Improved coastal wetland mapping using very-high 2-meter spatial resolution imagery. **International Journal Of Applied Earth Observation And Geoinformation**, [S.L.], v. 40, p. 11-18, ago. 2015. Elsevier BV. DOI: 10.1016/j.jag.2015.03.011

MCFEETERS, S. K. The use of the Normalized Difference Water Index (NDWI) in the delineation of open water features. **International journal of remote sensing**, v. 17, n. 7, p. 1425-1432, 1996. DOI: 10.1080/01431169608948714.

MEDDE, E. T.; BERTHIER, L.; BARDY, M.; CHENU, J. P.; GUZMOVA, L.; LAROCHE, B. Enveloppes des milieux potentiellement humides de la France métropolitaine. **Programme de modélisation des milieux potentiellement humides de France. Ministere d'Ecologie, du Développement Durable et de l'Energie, Rennes, France**, 2014.

MEROT, P.; HUBERT-MOY, L.; GASCUEL-ODOUX, C.; CLEMENT, B.; DURAND, P.; BAUDRY, J.; THENAIL, C. A Method for Improving the Management of Controversial Wetland. **Environmental Management**, [S.L.], v. 37, n. 2, p. 258-270, 4 nov. 2005. Springer Science and Business Media LLC. DOI: 10.1007/s00267-004-0391-4

MOOMAW, W. R.; CHMURA, G. L.; DAVIES, G. T.; FINLAYSON, C. M.; MIDDLETON, B. A.; NATALI, S. M.; SUTTON-GRIER, A. E. Wetlands In a Changing Climate: science, policy and management. **Wetlands**, [S.L.], v. 38, n. 2, p. 183-205, abr. 2018. Springer Science and Business Media LLC. DOI: 10.1007/s13157-018-1023-8.

MOREIRA, A. A.; FASSONI-ANDRADE, A. C.; RUHOFF, A. L.; PAIVA, R. C. D. REMOTE SENSING OF WATER BALANCE IN PANTANAL. **Raega - O Espaço Geográfico em Análise**, [S.L.], v. 46, n. 3, p. 20, 28 ago. 2019. Universidade Federal do Paraná. DOI: 10.5380/raega.v46i3.67096.

PEKEL, J. F.; COTTAM, A.; GORELICK, N.; BELWARD, A. S. High-resolution mapping of global surface water and its long-term changes. **Nature**, [S.L.], v. 540, n. 7633, p. 418-422, 7 dez. 2016. Springer Science and Business Media LLC. DOI:10.1038/nature20584.

PETIT, S.; STASOLLA, M.; WYARD, C.; SWINNEN, G.; NEYT, X.; HALLOT, E. A New Earth Observation Service Based on Sentinel-1 and Sentinel-2 Time Series for the Monitoring of Redevelopment Sites in Wallonia, Belgium. **Land**, [S.L.], v. 11, n. 3, p. 360, 1 mar. 2022. MDPI AG. DOI: 10.3390/land11030360.

RAPINEL, S.; FABRE, E.; DUFOUR, S.; ARVOR, D.; MONY, C.; HUBERT-MOY, L. Mapping potential, existing and efficient wetlands using free remote sensing data. **Journal Of Environmental Management**, [S.L.], v. 247, p. 829-839, out. 2019. Elsevier BV. DOI: 10.1016/j.jenvman.2019.06.098.

RIBEIRO, S.; MOREIRA, L. F. B.; OVERBECK, G. E.; MALTCHIK, L. Protected Areas of the Pampa biome presented land use incompatible with conservation purposes. **Journal Of Land Use Science**, [S.L.], v. 16, n. 3, p. 260-272, 4 maio 2021. Informa UK Limited. DOI: 10.1080/1747423X.2021.1934134.

RIO GRANDE DO SUL. Secretary of Planning, Governance and Management. Department of Government Planning Socioeconomic **Atlas of Rio Grande do Sul/Rio Grande do Sul**. 6. Ed. – Porto Alegre, 2021. 203 p.: il.

ROLON, A. S.; ROCHA, O.; MALTCHIK, L. Diversidade de macrófitas aquáticas do Parque Nacional da Lagoa do Peixe. **Neotropical Biology And Conservation**, [S.L.], v. 6, n. 1, p. 5-12, 11 maio 2011. Pensoft Publishers. DOI: 10.4013/nbc.2011.61.02.

ROUSE, J. W.; HAAS, R. H.; SCHELL, J. A.; DEERING, D. W. Monitoring vegetation systems in the Great Plains with ERTS. **NASA Spec. Publ**, v. 351, n. 1, p. 309, 1973.

RUBEC, C. The Canadian Wetland Classification System. **The Wetland Book**, [S.L.], p. 1577-1581, 2018. Springer Netherlands. DOI: 10.1007/978-90-481-9659-3_340.

RUIZ, L. F. C.; GUASSELLI, L .A.; SIMIONI, J. P. D.; BELLOLI, T. F.; FERNANDES, P. C. B. Object-based classification of vegetation species in a subtropical wetland using Sentinel-1 and Sentinel-2A images. **Science Of Remote Sensing**, [S.L.], v. 3, p. 100017, jun. 2021. Elsevier BV.DOI: 10.1016/j.srs.2021.100017.

SALINAS, J. B. G;. EGGERTH, M. K. P;. MILLER, M. E; MEZA, R. R. B; CHACALTANA, J. T. A;. ACUÑA, J. R;. BARROSO, G. F. Wetland mapping with multitemporal Sentinel Radar remote sensing In the southeast region of Brazil. In: **2020 IEEE Latin American GRSS & ISPRS Remote Sensing Conference (LAGIRS)**. IEEE, 2020. p. 669-674. DOI: 10.1109/LAGIRS48042.2020.9165593.

SCHÄFER, A.; LANZER, R.; SCUR, L. Atlas socioambiental dos municípios de Cidreira, Balneário Pinhal, Palmares do Sul. **EDUCS, Caxias do Sul**, 2013, v., p. 14-22.

SCHUH, M. H.; GUADAGNIN, D. L. Habitat and landscape factors associated with the nestedness of waterbird assemblages and wetland habitats in South Brazil. **Austral Ecology**, [S.L.], v. 43, n. 8, p. 989-999, 25 jul. 2018. Wiley. DOI:10.1111/aec.12648.

SCOTT, D. A.; JONES, T. A. Classification and inventory of wetlands: A global overview. **Vegetatio**, v. 118, n. 1-2, p. 3-16, 1995.

SEMENIUK, C. A.; SEMENIUK, V. A comprehensive classification of inland wetlands of Western Australia using the geomorphic-hydrologic approach. **Journal of the Royal Society of Western Australia**, v. 94, n. 3, p. 449, 2011.

SEMENIUK, C. A.; SEMENIUK, V. A geomorphic approach to global classification for inland wetlands. **Vegetatio**, [S.L.], v. 118, n. 1-2, p. 103-124, jun. 1995. Springer Science and Business Media LLC. . DOI: 10.1007/BF00045193.

SIMIONI, J. P.; GUASSELLI, L. A.; OLIVEIRA, G.; MATAVELI, G. A. V.; SANTOS, T. V Remote

Sensing-Based Method to Assess Water Level Fluctuations in Wetlands in Southern Brazil. **Geohazards**, [S.L.], v. 1, n. 1, p. 20-30, 12 maio 2020. MDPI AG. DOI:10.3390/geohazards1010003.

SIMIONI, J. P. D; GUASSELLI, L. A.; DE OLIVEIRA, G. G. A.; RUIZ, L. F. C.; OLIVEIRA, G. A comparison of data mining techniques and multi-sensor analysis for inland marshes delineation. **Wetlands Ecology And Management**, [S.L.], v. 28, n. 4, p. 577-594, 8 jun. 2020. Springer Science and Business Media LLC. DOI: 10.1007/s11273-020-09731-2

SMARDON, R. Wetlands and Sustainability. **Water**, [S.L.], v. 6, n. 12, p. 3724-3726, 28 nov. 2014. MDPI AG. DOI: 10.3390/w6123724.

SMITH R, D.; AMMANN A.; BARTOLDUS, C.; BRINSON, M. M. An approach for assessing wetland functions using hydrogeomorphic classification, reference wetlands, and functional indices. Publisher, **U.S. Army Engineer Waterways Experiment Station**, 1995.

SOUZA, C. M.; SHIMBO, J. Z.; ROSA, M. R.; PARENTE, L. L.; ALENCAR, A. A.; RUDORFF, B. F. T.; HASENACK, H.; MATSUMOTO, M.; FERREIRA, L. G.; SOUZA-FILHO, P. W. M. Reconstructing Three Decades of Land Use and Land Cover Changes in Brazilian Biomes with Landsat Archive and Earth Engine. **Remote Sensing**, [S.L.], v. 12, n. 17, p. 2735, 25 ago. 2020. MDPI AG. DOI: 10.3390/rs12172735.

STATE SECRETARIAT FOR THE ENVIRONMENT OF RIO GRANDE DO SUL (SEMA). **FEPAM Digital Cartographic Base**, Wetlands, 1:250,000. DIGITAL LIBRARY, 2013. Available at <http://www.fepam.rs.gov.br/biblioteca/geo/bases_geo.asp>

STATE SECRETARIAT FOR THE ENVIRONMENT OF RIO GRANDE DO SUL (SEMA). **SEMA Digital Cartographic Database, Hydrography, Wetlands**, 2018, Scale 1: 25,000. Available at <http://ww2.fepam.rs.gov.br/bcrs25/>.

STEYAERT, P.; BARZMAN, M.; BILLAUD, J.; BRIVES, H.; HUBERT, B.; OLLIVIER, G.; ROCHE, B. The role of knowledge and research in facilitating social learning among stakeholders in natural resources management in the French Atlantic coastal wetlands. **Environmental Science & Policy**, [S.L.], v. 10, n. 6, p. 537-550, out. 2007. Elsevier BV. DOI: 10.1016/j.envsci.2007.01.012.

SUERTEGARAY, D. M. A.; GUASSELLI, L .A. Landscapes (images and representations) of Rio Grande do Sul. In **Rio Grande do Sul: landscapes and territories in transformation.** Org. Verdum, R.; Basso, L.A.; 2ed.Porto Alegre: UFRGS Editora, 2012, v. , p. 27-38, 360p.

TASSI, A.; VIZZARI, M. Object-Oriented LULC Classification in Google Earth Engine Combining SNIC, GLCM, and Machine Learning Algorithms. **Remote Sensing**, [S.L.], v. 12, n. 22, p. 3776, 17 nov. 2020. MDPI AG. DOI: 10.3390/rs12223776.

TINER, R. W. Wetland Indicators: A Guide to Wetland Identification, Delineation, Classification, and Mapping. **Boca Raton: CRC Press LLC**,1999. 418 p. DOI: 10.1201/9781420048612.

TINER, R. W.; LANG, M. W.; KLEMAS, V. V. Remote Sensing of Wetlands: Applications and Advances; **CRC Press: Boca Raton,** FL, USA, 2015. DOI: 10.1201/b18210.

TOMAZELLI, L. J.; VILLWOCK, J. A. O Cenozóico do Rio grande do Sul: Geologia da Planície Costeira. Holz, M & DeRos, LF. **Geologia do Rio Grande do Sul**, 2000.

U. S. GEOLOGICAL SURVEY/NASA - **USGS 2018** - MOD16A2 v006. Available in: https://lpdaac.usgs.gov/products/mod16a2v006/.

VALENTI, V. L.; CARCELEN, E. C.; LANGE, K.; RUSSO, N. J.; CHAPMAN, B. Leveraging Google Earth Engine User Interface for Semiautomated Wetland Classification in the Great Lakes Basin at 10 m With Optical and Radar Geospatial Datasets. **Ieee Journal Of Selected Topics In Applied Earth Observations And Remote Sensing**, [S.L.], v. 13, p. 6008-6018, 2020. Institute of Electrical and Electronics Engineers (IEEE). DOI: 10.1109/JSTARS.2020.3023901.

VILLWOCK, J. A.; TOMAZELLI, L. J. TÉCNICAS, Notas. Geologia costeira do Rio Grande do sul. **Notas técnicas**, v. 8, p. 1-45, 1995.

VILLWOCK, J. A.; TOMAZELLI, L. J.; LOSS, E.L.; DENHARDT, E. A.; HORN FILHO, N. O.; BACHI, F.

A.; DENHARDT, B. A. Geology of the Rio Grande do Sul province. In: Rabassa, J. (ed.), International Symposium on Sea Level Changes and Quaternary Shorelines, São Paulo. **Quaternary of South America and Antarctic Peninsula. Balkema**: Rotterdam, v.4, p79-97, 1986.

VOLK, M.; HOCTOR, T. S.; NETTLES, B. B.; HILSENBECK, R.; PUTZ, F. E.; OETTING, J. Florida land use and land cover change in the past 100 years. **Florida's Climate: Changes, Variations, & Impacts**, 2017. DOI: 10.17125/fci2017.ch02.

WU, Q.; LANE, C. R.; LI, X.; ZHAO, K.; ZHOU, Y.; CLINTON, N.; DEVRIES, B.; GOLDEN, H. E.; LANG, M. W. Integrating LiDAR data and multi-temporal aerial imagery to map wetland inundation dynamics using Google Earth Engine. **Remote Sensing Of Environment**, [S.L.], v. 228, p. 1-13, jul. 2019. Elsevier BV. DOI: 10.1016/j.rse.2019.04.015.

WU, Y.; XI, Yi; FENG, M.; PENG, S. Wetlands Cool Land Surface Temperature in Tropical Regions but Warm in Boreal Regions. **Remote Sensing**, [S.L.], v. 13, n. 8, p. 1439, 8 abr. 2021. MDPI AG. DOI: 10.3390/rs13081439.

XU, H. A study on information extraction of water body with the modified normalized difference water index (MNDWI). **JOURNAL OF REMOTE SENSING-BEIJING-**, v. 9, n. 5, p. 595, 2005.

ZANOTTA, D, ZORTEA, M, FERREIRA, M, P. **Processamento de imagens de satélite**. Edição 1. São Paulo: Oficina de Textos, 2019.

ZOOBOTANICAL FOUNDATION OF RIO GRANDE DO SUL (FZB). **Mapping of wetlands, Digital files for use in GIS** - RS digital cartographic base 1:250.000, 2013. Available in <http://www.fepam.rs.gov.br/biblioteca/geo/bases_geo.asp>.

ZOU, Y.; WANG, L.; XUE, Z; E, M.; JIANG, M.; LU, X.; YANG, S.; SHEN, X.; LIU, Z.; SUN, G. Impacts of Agricultural and Reclamation Practices on Wetlands in the Amur River Basin, Northeastern China. **Wetlands**, [S.L.], v. 38, n. 2, p. 383-389, 22 nov. 2017. Springer Science and Business Media LLC. DOI: 10.1007/s13157-017-0975-4.

First author biograohy

Christhian Santana Cunha, originally from São Gabriel, RS-Brazil, was born on January 12, 1989. He holds a Bachelor's degree in Environmental Management from the Federal University of Pampa (UNIPAMPA). He also has a Master's degree in Civil Engineering with a concentration in Water Resources and Environmental Sanitation from the Federal University of Santa Maria (UFSM). Currently, he is a Ph.D. candidate in the Remote Sensing Graduate Program at the Federal University of Rio Grande do Sul (UFRGS) and is a member of the Geoprocessing and Environmental Analysis Laboratory – LAGAM. He is involved in research related to the mapping of wetland areas and water resources.